International Journal of Physics
and Research (IJPR)
ISSN(P): 2250-0030; ISSN(E): 2319-4499
Vol. 4, Issue 5, Oct 2014, 19-28

EFFECT OF REACTIVE METAL ON CREEP RESISTANCE OF SN-50BI LEAD FREE SOLDER ALLOYS

MUSTAFA KAMAL & RIZK MOSTAFA SHALABY

Metal Physics Laboratory, Department of Physics, Faculty of Science, Mansoura University, Mansoura, Egypt

ABSTRACT

Sn-Bi alloy is an attractive soldering material for temperature- sensitive electronic device. With its excellent creep resistance and fracture resistance, Sn-Bi alloy has become one of the promising candidates to replace Pb-based solders. The x-ray diffraction results show that the structure of Sn_{100-x}-50Bi-xNi (x=0, 0.1, 0.3 and 0.5 wt.%) alloys characterized by the presence of rhombohedral Bi and body centered tetragonal β-Sn. The addition of nickel to the Sn-50Bi binary system lowers the melting temperature. In this study low concentration of reactive metal, i.e., Ni, has been added into the Sn-50Bi alloy to enhance the creep resistance. Effective enhance of the creep resistance was attributed to solid-solution and precipitation strengthening effects by the Bi addition residing in the Sn-rich phase. Sn-Bi solid solutions with Ni concentrations up to 1.0 wt. % show significant higher hardness and elastic modulus that delays the fracture because of grain size refinement. The strain-time relationship of the ternary Sn-Bi-Ni alloys have been evaluated in the range from 5 to 99s at constant load = 0.098 N.

KEYWORDS: Sn-Bi-Ni, Hardness, Fracture, Mechanical Properties, Creep Resistance

INTRODUCTION

Sn-Bi, has superior fracture resistance, yield strength and comparable solderability with Sn-Pb alloy [1]. It has drawn great research focus as potential replacement for Pb-containing solders in the microelectronic industry. Its low melting point (T_m=139 ˚C at eutectic concentration) could effectively reduce the thermal stress built-up at the electronic joints during the multiple reflow processes. Lu Shen et al. [2] has investigated nano-indentation study on the creep resistance of Sn-Bi solder alloy with reactive nano-metallic fillers. In their study, low concentration of reactive nano-metallic fillers, i.e., Cu and Ni, have been added into the Sn-58Bi alloy.The elastic, plastic and creep properties are characterized by nano-indentation constant strain rate technique. The addition of the fillers has refined the microstructure of the solder matrix leading to moderate strengthening and hardening. One potential method for improving joint reliability is to use a lower-melting point solder alloy. Sn-Bi solder alloy as low-temperature lead free-solder was used extensively because of its low-melting point (the melting points of the Sn-50Bi solder alloy is 412 k), high tensile strength and excellent creep resistance [3]. However, previous studies indicated that the poor ductility, grain coarsening during thermal aging reduced the mechanical properties of the Sn-Bi solder alloy [4]. Several reports show that Ag and Cu additions refined the microstructure of Sn-Bi solder alloy [5-9]. Effect of silver and indium addition on mechanical properties and indentation creep behavior of rapidly solidified Bi-Sn based lead free solder was studied by [10] and compared to that of the traditional Sn-37 wt.%Pb eutectic alloy. The results show that the In and Ag containing solder alloy exhibited a good combination of higher creep resistance, good mechanical properties and lower melting temperature as compared with Pb-Sn eutectic solder alloy. Creep behavior of the lead-free Sn-Bi alloys with bismuth contents in the range of 1-5 wt.%

was studied by long time Vickers indentation testing at room temperature [11]. The stress exponents were determined through the application of different indentation methods. The exponents of 13.4-15.3 and 9.2-10.0 have been respectively found for the cast and wrought conditions. The effect of trace amounts of trace earth additions on the microstructure and properties were studied for the Sn-58 Bi and Sn-58Bi-Ag solder alloys [12]. The results indicate that adding trace amounts of rate earth (RE) elements has little influence on the melting temperature and microhardness of the solders investigated, but adding RE elements improves the wettability, and shear strength of the Sn-58Bi and Sn-58Bi-Ag solder alloys. In addition, it was found that the addition of RE elements not only refines the microstructure and size of the IMC particles but also decreases the IMC thickness and shear strength of the Sn-58Bi solder joint after high temperature aging. Adding trace amounts of RE elements is superior to adding trace amounts of Ag for improving the properties of the Sn-58Bi solder. Creep behavior of the Sn-2Bi-RE alloys containing 0.1, 0.25 and 0.5 wt.% rare earth (RE) elements was started by impression testing and compared to that of the Sn-2Bi alloy. Results showed that, Sn-2Bi-0.25RE alloy had the lowest creep rate, and thus the highest creep resistance among all materials tested [13]. In the present study, five types of solder alloys Sn-$Bi_{50-x}Ni_x$ (x=0, 0.1, 0.3, 0.5 and 1.0) were adopted to investigate the effect of different amounts of Ni additions on the fracture and mechanical properties of Sn-50Bi solder alloys.

EXPERIMENTAL

Materials and Sample Preparation

The materials under evaluation in this study are Sn-Bi_{50-x}-Ni_x alloys with values of x=0, 0.1, 0.3, 0.5 and 1.0 wt.%. The corresponding concentration of the Sn-50Bi alloy is displayed as line (a) in the binary phase diagram and it represents the hypo-eutectic concentration [our study] as shown in Figure 1 [14] while line (b) represents the eutectic composition. The alloy samples were prepared by mixing appropriate amount of pure Sn, pure Bi and pure Ni particles (commercially available with purity >99.9 %) with total weight of approximately 20 gm. The mixture was then melted at 500 ˚C (enough to dissolve (0.1, 0.3, 0.5, and 1 wt.% Ni) as this small amount of Ni dissolves in the master alloy according to phase diagram), then by ejecting the molten alloys on a rotating copper wheal (2900 rpm) which corresponds to a linear speed of 31.4 m/sec of the melt-spinning technique. The resulting alloys have long ribbons from 100 μm in thickness to 1 cm width. The density value of the solder alloys was determined in the present work as shown in Table 1.

Table 1: Calculated and Experimental Densities, d, of the Prepared Alloys

Alloy	d_{calc} gm/cm^3	$d_{exp.}$ gm/cm^3
Sn-50Bi	8.547	8.511
Sn-49.9Bi-0.1Ni	8.542	8.522
Sn-49.7Bi-0.3Ni	8.542	8.488
Sn-49.5Bi-0.5Ni	8.522	8.435
Sn-49.0Bi-1.0 Ni	8.497	8.413

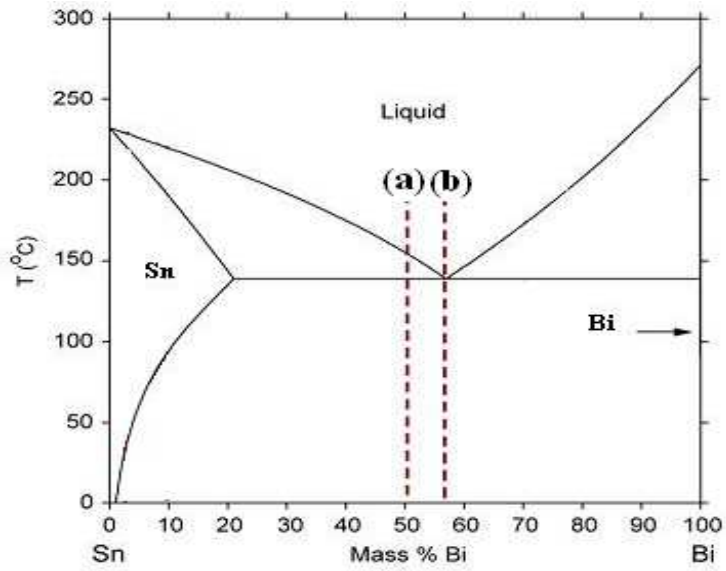

Figure 1: Phase Diagram of Sn-Bi System, Demonstrate the Concentration Evaluated in this Study

Structural and Thermal Studies

The structure of the samples was studied by x-ray diffractometer (XRD, X pert PRO, PANalytical using Cuk_{α} target with secondary monochromator) was used to identify the structure of all samples. Differential scanning calorimatery is carried out by (DSC-16, Setaram, France) with a heating rate 10 K/min.

Elastic Modulus and Indentation Measurement

The dynamic Young's modulus was examined by a dynamic resonance technique from the resonance curve after determination of the resonance frequency. The produced samples were tested in a Vickers microhardness tester, where a diamond pyramid indenter with square base is used and the Vickers hardness number is given by $H_v=0.185\ F/d^2$, where F is the applied load in N and d, is the average diagonal length in mm. Each reading was an average of at least ten measurements on the surface of the specimens. Micro-creep measurements as described elsewhere [15, 16] were also carried out using a Vickers hardness tester using a fixed load of 0.098 N for dwell time up to 99 s.

RESULTS AND DISCUSSIONS

Phase Designation

Figure 2 shows the properties of XRD patterns for the Sn-50Bi, Sn-49.9Bi-0.1Ni, Sn-49.7Bi-0.3Ni, Sn-49.5Bi-0.5Ni and Sn-49Bi-1.0Ni solder alloys. The alloys of Sn-50Bi and $Sn\text{-}Bi_{50-x}\text{-}Ni_x$ (x=0.1, 0.3, 0.5 and 1.0 wt.%) consists of two phases; rhombohedra (R-3m) Bi rich phase matrix and body centered tetragonal β-Sn phase respectively. The Sn-Bi phase diagram shows that solubility of Bi in Sn is only about 2 mass % at room temperature [14]. In the case of adding 0.1 wt.% Nickel (Ni) to Sn-50Bi alloy, the pattern shows the same phases with increasing the intensity of x-ray diffraction peaks due to Bi which means decreasing the solubility of Bi in Sn-matrix. Also, there isn't any peak characteristic due to Ni phase which means a complete solubility of Ni in Sn matrix for all ternary alloys. The solubility of Ni in the Sn-matrix causes a small shift of the x-ray diffraction peaks to lower angles. The angular shift indicates the increase of the lattice parameter (a) of the tetragonal Sn-matrix, as illustrated in Figure 2, which can be attributed to the lower atomic radius of Ni and Bi atoms compared to Sn atoms [17]. Lattice constants of β-Sn for different compositions are shown in Table 2. The lattice parameters of β-Sn decreases with Ni content in solid solution and the size of the

decreases has been suggested to be related to the closest distance constituent atoms.

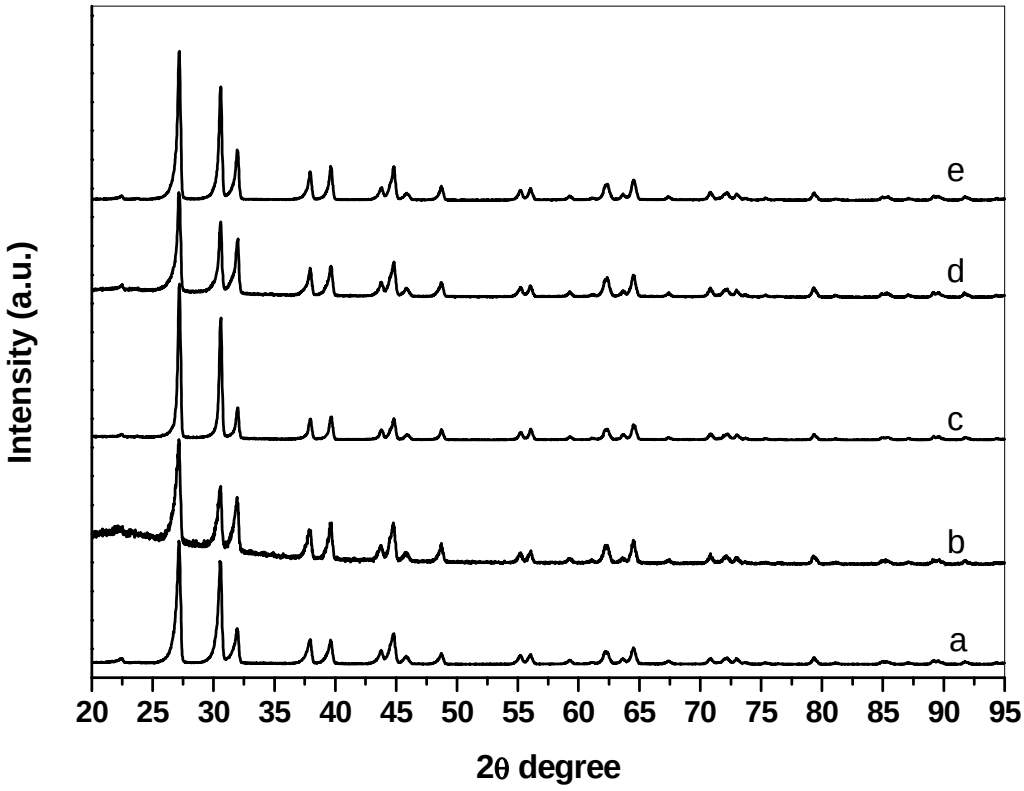

Figure 2: The XRD Patterns of Melt-Spun: (a) Sn-50Bi, (b) Sn-49.9Bi-0.1Ni, (c) Sn-49.7Bi-0.3Ni, (d) Sn-49.5Bi-0.5Ni and (d) Sn-49Bi-1.0Ni

Table 2: Details of the X-Ray Diffraction Analysis (XRD) of Sn-Bi-Ni Lead-Free Solder Alloys

Alloy	a Å	c Å	c/a	Grain Size µm	Phase Designation
Sn-50Bi	5.842	3.188	0.5457	477.14	tetragonal β-Sn rhombohedra Bi
Sn-49.9Bi-0.1Ni	5.852	3.1945	0.5458	387.13	tetragonal β-Sn rhombohedra Bi
Sn-49.7Bi-0.3Ni	5.8489	3.1929	0.5459	364.21	tetragonal β-Sn rhombohedra Bi
Sn-49.5Bi-0.5Ni	5.849	3.1949	0.5462	357.11	tetragonal β-Sn rhombohedra Bi
Sn-49.0Bi-1.0 Ni	5.8436	3.1925	0.5463	244.71	tetragonal β-Sn rhombohedra Bi

Melting Behavior of Sn-Bi-Ni Lead-Free Solder Alloys

Melting temperature is a critical solder characteristic, because it determines the maximum operating temperature of the system and the minimum processing temperature of its components must survive. Table 3 gives the melting temperatures of some solder alloys with melting points below 232 ˚C (the melting temperature of Sn) that contains niether Pb nor Cd, which is even more toxic [18-20]. All compositions are given in weight percent. The defferential scanning calorimetry (DSC) curves obtained for the binary and ternary alloys during heating with heating rate 10 K/min are shown in Figure 3. The figure for all prepared alloys shows a single exothermic peak corresponding to the melting reaction.

From this figure the melting point (T_m), solidus temperatutere (T_s), Liquidus temperature (T_l), Enthalpy of fusion (ΔH_f) and pasty range of these alloys were calculated and presented in Table 3. The nickel substitution of 1 % by weight for Sn in the Sn-50Bi was found to reduce the melting temperature by 3 ˚C, from 143.62 ˚C to 140.78 ˚C so that alloy melts at a temperature about 3 ˚C smaller than that of Sn-50Bi solder (143.62 ˚C). The melting point decreases continously with small Ni content up to 140.78 ˚C at Sn-49Bi-1.0Ni alloy. This reduction may be attributed to the decrease of the crystalline size, as observed in the work of Peter et al. [21]. The lower value of the enthalpy of fusion for 1 wt.% Ni, may be due to the presence of some precipitates of Bi and Ni in Sn matrix. The pasty range (the solidus-liquidus distance), which is the range between the solidus and liquidus temperatures, for the Sn-49wt.%Bi-1 wt.%Ni is equal to 8.34˚C, while for the other alloys exhibits a positive increase up to 9.15 ˚C.

Table 3: Melting Temperature(T_m), Solidus Temperature (T_s), Liquidus Temperature (T_l), Pasty Range (T_{end}-T_{onset}), and Enthalpy for Five Solder Alloys

Alloy	T_m (˚C)	Onset Point (˚C)	Endset Point (˚C)	Pasty Range (˚C)	Enthalpy µv.s/mg
Sn-50Bi	143.62	141.35	150.50	9.15	14.3467
Sn-49.9Bi-0.1Ni	143.22	140.52	149.50	8.98	14.234
Sn-49.7Bi-0.3Ni	142.35	139.53	148.39	8.86	13.245
Sn-49.5Bi-0.5Ni	141.33	138.66	147.58	8.92	12.435
Sn-49Bi-1.0Ni	140.78	138.23	146.57	8.34	11.8207

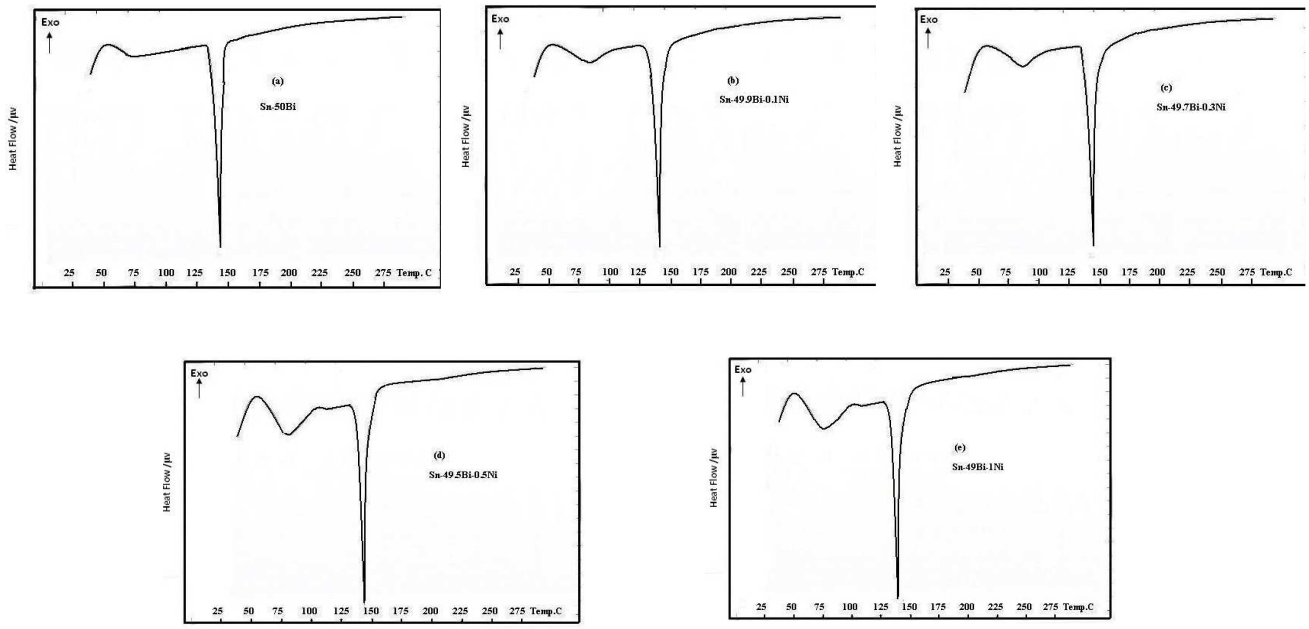

Figure 3: Differential Scanning Calorimatry (DSC) Curves of the Five Lead Free Solder Alloys Upon Heating at a Scaninnig Rate of 10 K/min.; (a) Sn-50Bi, (b) Sn-49.9Bi-0.1Ni, (c) Sn-49.7Bi-0.3Ni, (d) Sn-49.5Bi-0.5Ni, and (e) Sn-49Bi-1.0Ni

Elastic Modulus of SnBiNi Alloys

Table 4 shows the modulus results of the Sn-Bi alloys with different concentration of Ni. Pure Sn and Bi, with modulus of 44.62 GPa and 25.89 GPa respectively, are included for comparison. Among all the samples being evaluated, Sn–49 Bi -1.0Ni has the highest modulus of 52.69 GPa followed by Sn–49.5Bi-0.5Ni. The enhancement of the stiffness from Sn-Bi to that Sn-49Bi- 1%Ni is attributed to the presence of Bi precipitates and Ni atoms are fully dissolved in the Sn

lattice. In Sn–50%Bi sample, the Sn-rich phase contains the maximum solubility of Bi (3 wt. %). However, the stiffness of the Sn-50Bi alloy has been decreased compared with Sn–49Bi-1.0Ni due to the presence of non-soluble Bi precipitation aggregated at the Sn-rich phase. Decreasing the Bi content from 50 wt. % in the alloy has monotonically increased the over all modulus of the SnBiNi alloys. From SnBi phase diagram (Figure 1), it can be seen that the constituent phases of SnBi composites are Bi phase (with no solubility of Sn) and Sn-rich phase (with 3 wt. % Bi soluble at room temperature).

Table 4: Elastic Modulus (E), Hardness (H_v) and Yield Strength (Y) of Sn-Bi-Ni Lead Free Solder Alloys with Different Concentrations

Alloy	E GPa	0.098 N, 5 s	Hv MPa	1.96 N, 99 s	0.098 N, 5s	Y MPa	1.96 N, 99 s
			1.96 N, 5 s			1.96 N, 5 s	
Sn	44.62	250.45	200.12	180.98	83.48	66.70	60.32
Bi	25.89	320.23	280.23	260.23	106.74	93.41	86.74
Sn-50Bi	46.42	350.22	290.23	220.22	116.64	96.74	73.41
Sn-49.9Bi-0.1Ni	47.51	380.27	330.91	300.14	126.75	110.30	100.04
Sn-49.7Bi-0.3Ni	48.92	400.13	350.36	320.28	133.37	116.78	106.76
Sn-49.5Bi-0.5Ni	50.33	440.12	420.19	350.81	146.70	140.06	116.93
Sn-49.0Bi-1.0 Ni	52.69	500.31	450.17	410.91	166.77	150.05	136.97

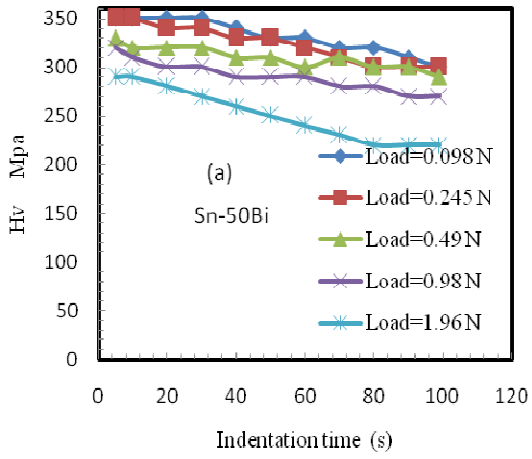

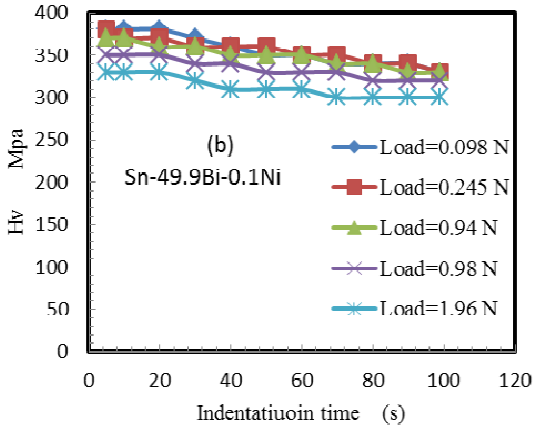

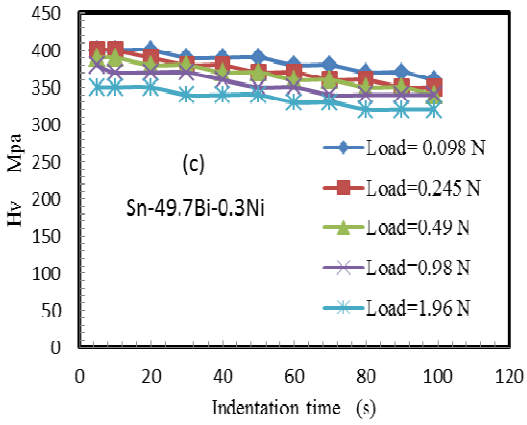

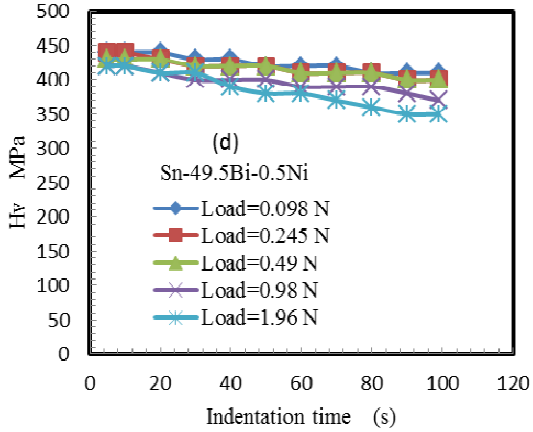

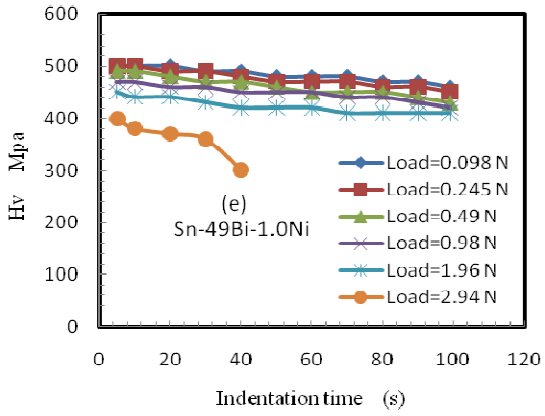

Figure 4: Variation of Vickers Microhardness with Indentation Time of Sn-(50-x)Bi-xNi Alloys

Hardness of SnBiNi Alloys

Resistance to plastic indentation is determined by an indentation hardness test, in which a small hard indenter is pressed into the surface by a standard load and the measured. In most tests a diamond indenter in the shape of a pyramid (Vickers test) is used. The hardness number H is defined as the load on the indenter divided by the area of contact between the indenter and the material usually given in $kgmm^{-2}$. Although the plastic indentation is not plane strain, the plastic constraint factor remains at about the same value, so that H≈3Y to a good approximation. This relation enables the hardness test to be used as a simple, cheep and non-destructive means of evaluating the yield strengths of metals, particularly for quality control during production and diamond indents, as it always produces a geometrically similar indentation proportional to the hardness of the material or the depth of the indentation. The experimental determinations involve the measurement of the time and load dependence of hardness in addition to the effect of Ni content on the binary Sn-50Bi alloys, Table 4. The values of hardness (Hv) and yield strength for Sn-Bi_{x-1}-Ni_x (x=0.0, 0.1, 0.2, 0.3, 0.5 and 1.0 wt. %) alloys are given in Table 4. It is clear that the hardness and yield strength increases with Ni additions up to a maximum value at 2 wt.% Ni. Figure 4 shows the variation of Vickers hardness number versus indentation time for Sn-Bi_{x-1}-Ni_x (x=0.0, 0.1, 0.2, 0.3, 0.5 and 1.0 wt. %) alloys tested at 0.098, 0.245, 0.49, 0.98, 1.96 and 2.94 N. It shows slow decrease of H_v with time. The four samples contain Ni have much higher hardness as compared to the free Ni alloys. The hardness of the Sn–49Bi-1.0Ni is measured to be 500 MPa, an eminent increment of 30% as compared to that of the Sn-50Bi. It is believed that the Bi solute effectively hinders the dislocation movement with in Sn bulk lattice. The greatest enhancement of hardness is achievable when Bi reaches its maximum solubility at the temperature of evaluation. In Sn–49%Bi-1.0Ni sample, the aggregated Bi precipitates at the grain boundaries are found to increase the hardness of the matrix dramatically to 500 MPa. These secondary precipitates play the role of hindering dislocation slip as well as the grain boundary movement. It shows that, the Vickers hardness number of all alloys varies non-linearly with dwell time in the same manner. This type of non-linear behavior agrees with the results observed in [12-15] and is known as the indentation size effect [17]. Figure 5 shows the variation of microhardness H_v with Ni content for different applied loads, 0.098, 1.96 and 2.94 N. The Vickers hardness number increases with increasing Ni content up to 500 MPa at 1.0 wt. % Ni. The increase of hardness number can be attributed to presence of some precipitates of Bi and Ni atoms in Sn rich matrix and refinement the grain size through the application of the rapid solidification technique. In Figure 4 a, and b the fracture happens at 5 s and 2.94 N, while in Figure 4c the fracture happens at 50 and 2.94 N. After addition, the Ni at 1.0 wt. % the fracture is delayed with increasing dwell time as shown in Figure 4c. This is attributed to the presence of some precipitates

of Bi and Ni atoms in Sn rich matrix and the refinement of the grain size through the application of the rapid solidification technique.

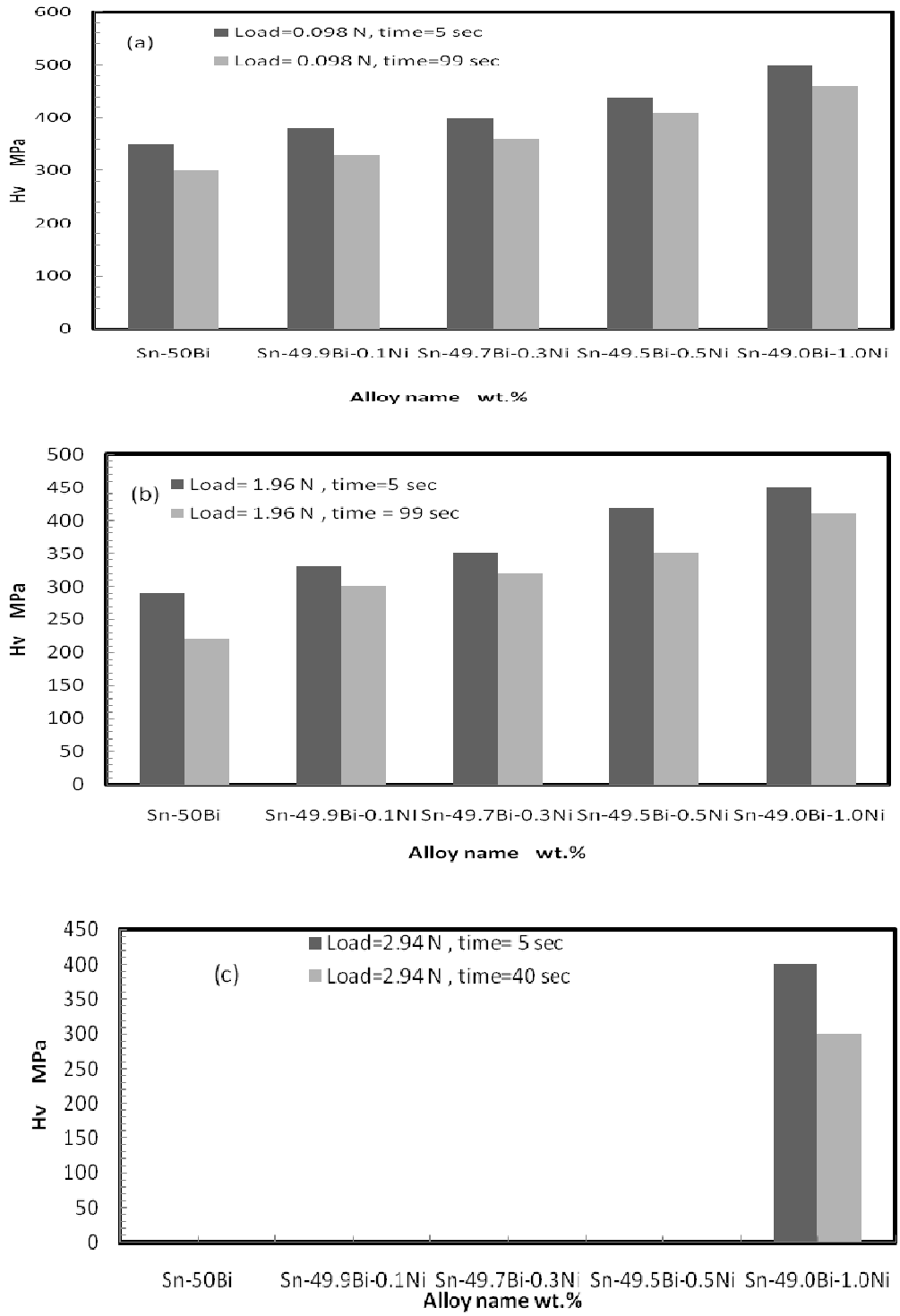

Figure 5: The Variation of Vickers Microhardness (H_v) with Nickel Content, a) Load = 0.098 N, t=5, 99 s, b) Load = 1.96 N, t=5, 99 s and c) Load=2.94 N, t= 5, 40 s

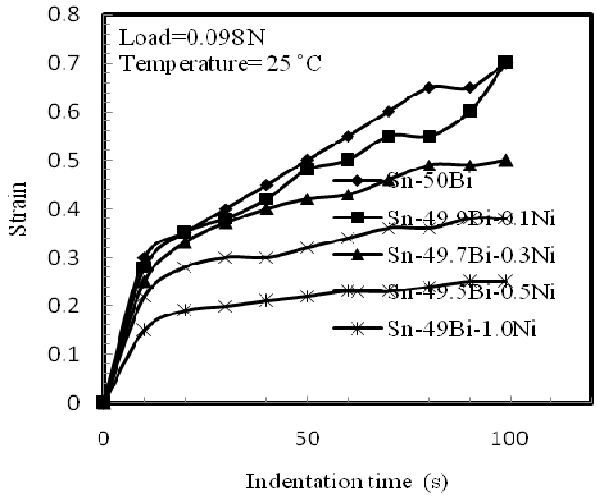

Figure 6: The Creep Behavior of Melt-Spun Sn-Bi-Ni Alloys

Creep Resistance

Figure 6 plots the strain and indentation time relationships of Sn-Bi-Ni in comparison with Sn-Bi. We obtain a typical creep curve, as shown in Figure 6. The first stage records a fast increase of strain with time of the indentation starts from beginning up to 10 s of indentation time. The second stage represents a slow increase region in which the strain increases by lower rates for all alloys. In general, Sn-Bi-Ni alloys have higher creep resistance than Sn-Bi alloy as lower creep rates are found in the alloys at same conditions. Sn-50Bi possesses the lowest creep rate followed by Sn-49.9Bi-0.1Ni. Alike the hardness behavior, Bi solid solute as well as the Bi precipitates in the Sn-rich phase attribute significantly to the enhancement of the creep resistance of the Sn matrix.

CONCLUSIONS

- From the results, it can be concluded that the formation of the two kinds of Sn-Bi phases is due to the addition of the traces of Ni into the Sn-Bi alloy which resulted in the refinement of the structure of the alloy and aid in its formation. It has shown considerable improvement in the mechanical properties of the alloy and delays the fracture because of grain size refinement. The addition of Ni also improved the tensile strength of Sn-Bi alloy.
- The addition of Ni has prolonged the creep-resistance of solder joint at room temperature. When the content of Ni is 1. 0 wt.%, the creep resistance was found to be 3 times or more than that of Sn-50Bi without Ni. When the content of Ni exceeded 0.1 wt.% it resulted in an increased creep-resistance of the solder joint. Effective enhancement of the creep resistance was attributed to solid-solution and precipitation strengthening effects by the Bi addition residing in the Sn-rich phase.

REFERENCES

1. F. Hua, Z. Mei, J. Glazer, in: 48th Electronic Components and Technology Conference, (1998) 227.
2. Lu Shen, Zheng Yu Tan, Zhong Chen, Mater. Sci. Eng. A, 561 (2013)232-238.
3. Z. Mei, J.W. Morris Jr., J.Electron. Mater., 21, (1992) 599.

4. S. Jin, M. McCormack, J. Electron. Mater., 23, 8, (1994) 735.
5. C. F. Peng, J. Shen, W. D.Xie, J.Chen, C.P. Wu, X.C. Wang, J. Mater. Sci.Mater. Electron., 22, 7, (2011) 797.
6. D.Q. Yu, L. Wang, C.M.L. Wu, C.M.T. Law, J. Alloys Compd., 389, (2005) 153.
7. J.F.Li, S.H.Mannan, M.P.Clode, K.Chen, D.C.Whalley, D.A.Hutt, Acta Mater., 55, 2, (2007) 737.
8. H.W.Miao, J.G.Duh, B.S.Chiou, J.Mater.Sci.: J. Mater. Electron., 11, (2000) 609.
9. C.M.L.Wu, D.Q.Yu, C.M.T.Law, L.Wang, Mater.Sci. Eng.R., 44, (2004) 1.
10. R.M.Shalaby, Mater.Sci. Eng. A 560 (2013) 86-95.
11. R.Mahmudi, A.R.Geranmayeh, S.R.Mahmudi, A.Khalatbari, J.Mater.Sci: Mater Electron (2007) 18, 1071-1078.
12. Wenxing Dong, Yaowu Shi, Zhidong Xia, Yongping Lie, Fu Guo, J. Elect. Mater, DOI: 10.1007/s11664 -008-0458-8, 2008.
13. R. Mahmudi, A.R. Geranmayeh, M. Salehi, H.Pirayesh, J.Mater.Sci: Mater. Electron., (2010) 21, 262-269.
14. M. Hansen, Constitution of Binary Alloys, McGraw-Hill, New York, 1958.
15. T.El. Ashram and R.M.Shalaby, J. Electron. Mater., 34, (2005) 212.
16. M. Kamal, A. El-Bediwi, A.R. Lashin, A.H. El-Zarka, Mater. Sci. Eng., A 530 (2011) 327-333.
17. J.C. Slater, Atomic radii in crystals, Chem. Phys. 41 (1964) 3199-3205.
18. P.G. Harris and M.A.Whitmore, Circuit World 19 (2), 25 (1993).
19. C. Melton, A.Skipor and J.Thome, Nepcon West.93, p.1489.
20. R.W. Wild. Tech. Rpt. 171200408, IBM Fedral Systems Division Laboratory, Owego NY 1971.
21. A. Peters, B. Chung, C. Cohen, Appl. Phys. Lett.71 (1997) 2391.